Identifying the Dominant Transmission Pathway in a Multi-stage Infection Model of the Emerging Fungal Pathogen *Batrachochytrium Salamandrivorans* on the Eastern Newt

Md Rafiul Islam, Matthew J. Gray, and Angela Peace

1 Introduction

Emerging infectious diseases are a threat to biodiversity and fungal pathogens have caused rapid declines in amphibian populations around the globe [18]. Gray et al. [6] identify *Batrachochytrium salamandrivorans* (Bsal) as an emerging fungal pathogen that caused rapid die-offs of naïve salamanders in Europe and predicts North America will soon experience similar devastation if no policy actions are taken and the pathogen emerges. Due to the fact that Bsal is such a recently emerging pathogen, we currently lack epidemiological data on how it may spread temporally and spatially across North America. Recent efforts have focused on building mathematical models to gain insight on pathogen spread and identify control strategies. Using Bsal as a case study, [8] employ Spatial Distribution Models to highlight the difficulty in validating model predictions when available data is limited, as well as the importance of appropriate model selection. Schmidt et al. [23] present a compartmental population model incorporating direct transmission and spatial diffusion that identified preventing emergence as the best strategy.

In order to better understand Bsal pathogen dynamics, we develop Susceptible-Infected-Recovered-Susceptible (SIRS) type disease models for a population of Eastern Newt adults. This particular species is widely distributed across eastern North America and has been shown to be highly susceptible to Bsal [17, 21]. In some cases, Bsal can lead to death in susceptible species within 2 to 3 weeks

M. R. Islam (✉) · A. Peace
Department of Mathematics and Statistics, Texas Tech University, Lubbock, TX, USA

Department of Mathematics, Iowa State University, Ames, IA, USA
e-mail: rafiul.islam@ttu.edu; rafiul@iastate.edu

M. J. Gray
Center for Wildlife Health, University of Tennessee Institute of Agriculture, Knoxville, TN, USA

M. I. Teboh-Ewungkem, G. A. Ngwa (eds.), *Infectious Diseases and Our Planet*,
Mathematics of Planet Earth 7, https://doi.org/10.1007/978-3-030-50826-5_7

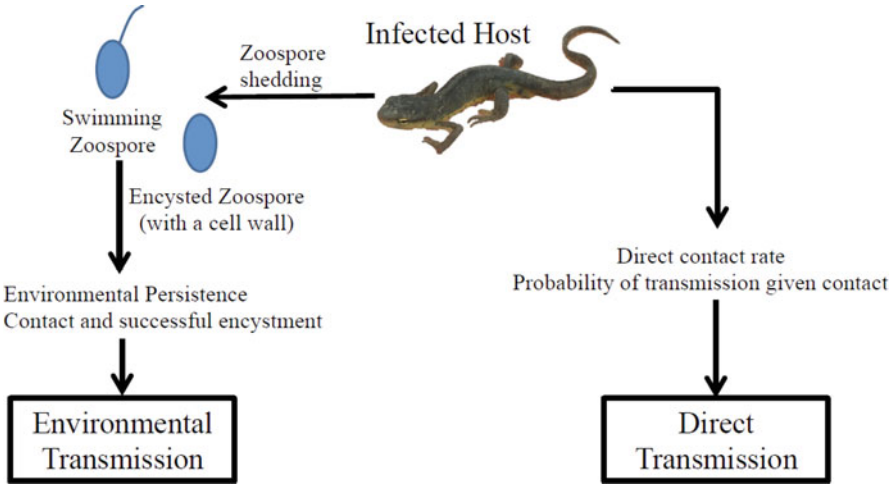

Fig. 1 Multiple transmission pathways

after exposure, but it has also been observed that some individuals can recover and clear the infection [17]. Compared to the duration of infection, adult Eastern Newts have a long lifespan potentially persisting >10 years [21, 22]. Unlike previous models [23], here we incorporate two routes of pathogen transmission: direct transmission via contact between infected and susceptible individuals and environmental transmission via shed zoospores in the water (Fig. 1). Bsal produces two types of zoospores that lead to environmental transmission, motile zoospores with flagellum and encysted zoospores with cell walls. Motile zoospores actively swim towards hosts, whereas encysted zoospores typically float on the surface [24].

We first present a base model that divides the host into four subpopulations depending on disease status (susceptible, latently infected, infectious, and recovered) as well as tracks the environmental loads of the two zoospores types. Epidemic compartmental models are commonly used to characterize the epidemiology of host–pathogen systems by providing means of estimating the invasion potential of a pathogen and surviving host population [9]. SIRS type models commonly assume that the duration of host infectiousness follows an exponential distribution [9], however, the duration of host infectiousness has been shown to be realistically closer related to a gamma-distributed [12, 25]. Following [25], we expand our base SIRS model to a full model that includes multiple stages of infection, each exponentially distributed so that the sum of the sequence of these independent exponentially distributed random variables approaches a gamma-distribution.

Since Bsal has not invaded North America yet, several parameter estimates remain unknown for eastern newts. For our simulations, we used a combination of Bsal data from eastern newts and European fire salamanders (Salamandra salamandra). We also used estimates of zoospore shedding from a closely related

chytrid species (B. dendrobatidis). We used sensitivity analyses to identify the most parameters driving transmission. In addition, by investigating the invasion probability (i.e., the basic reproduction number) we found that direct transmission is likely to be the dominant driver of pathogen dynamics for low density populations, whereas environmental transmission will dominate in high density populations.

2 Model Development

2.1 Base Model Development

We begin with a base model of ordinary differential equations where individuals are divided into four subpopulations, susceptible $S(t)$, latently infected but not infectious $L(t)$, infectious $I(t)$, and Recovered $R(t)$. Total population is denoted as $N(t) = S(t) + L(t) + I(t) + R(t)$. These state variables represent the density of individuals in an aquatic environment (e.g., pond), with units of number of individual per volume. Infected individuals shed two types of Bsal zoospores, $Z_m(t)$ and $Z_e(t)$ into the environment. These state variables have units of zoospore per volume. The schematic of the base model is shown in Fig. 2 and the equations take the following form:

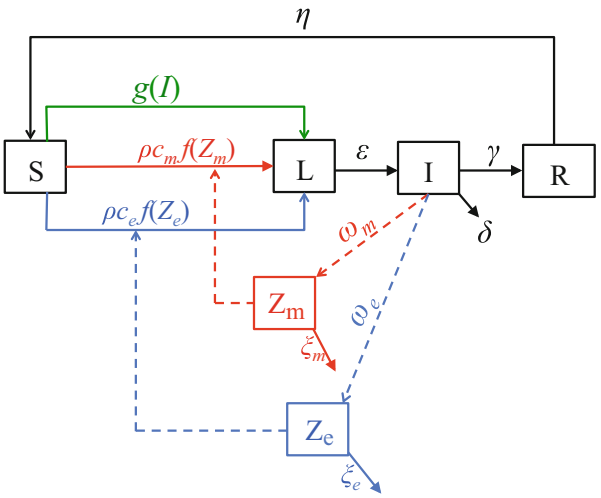

Fig. 2 Structure of the base model (1). The model tracks individuals divided into four subpopulations, susceptible $S(t)$, latently infected $L(t)$, infectious $I(t)$, and recovered $R(t)$, as well as the zoospores in the environment $Z_m(t)$ and $Z_e(t)$. The different routes of transmission are depicted using different colors, Direct transmission route is green, environmental transmission from Z_e is in blue, and from Z_m is in red. Solids lines depict the movement of individuals between compartments and dashed lines show the role of environmental zoospores

$$\frac{dS}{dt} = \underbrace{-g(I)S}_{\substack{\text{direct}\\ \text{transmission}}} \underbrace{-\rho(c_m f(Z_m,\kappa_m) + c_e f(Z_e,\kappa_e))S}_{\substack{\text{waterborne}\\ \text{transmission}}} + \underbrace{\eta R}_{\substack{\text{loss of}\\ \text{immunity}}} \tag{1a}$$

$$\frac{dL}{dt} = \underbrace{g(I)\,S}_{\substack{\text{direct}\\ \text{transmission}}} + \underbrace{\rho(c_m f(Z_m,\kappa_m) + c_e f(Z_e,\kappa_e))S}_{\substack{\text{waterborne}\\ \text{transmission}}} - \underbrace{\epsilon L}_{\substack{\text{latent becomes}\\ \text{infectious}}} \tag{1b}$$

$$\frac{dI}{dt} = \underbrace{\epsilon L}_{\substack{\text{latent becomes}\\ \text{infectious}}} - \underbrace{\delta I}_{\substack{\text{Bsal induced}\\ \text{death}}} - \underbrace{\gamma I}_{\substack{\text{Bsal}\\ \text{recovery}}} \tag{1c}$$

$$\frac{dR}{dt} = \underbrace{\gamma I}_{\substack{\text{recovery}\\ \text{rate}}} - \underbrace{\eta R}_{\substack{\text{loss of}\\ \text{immunity}}} \tag{1d}$$

$$\frac{dZ_m}{dt} = \underbrace{\omega_m I}_{\substack{\text{shed zoospores}\\ \text{type m}}} - \underbrace{\xi_m Z_m}_{\substack{\text{Bsal degradation}\\ \text{for zoospores type m}}} \tag{1e}$$

$$\frac{dZ_e}{dt} = \underbrace{\omega_e I}_{\substack{\text{shed zoospores}\\ \text{type e}}} - \underbrace{\xi_e Z_e}_{\substack{\text{Bsal degradation}\\ \text{for zoospores type e}}}. \tag{1f}$$

Susceptible individuals can become latently infected after contact with an infected individual following direct transmission rate given by function $g(I)$. Here, we consider both frequency-dependent and density-dependent direct transmission rates:

$$g(I) = \beta\frac{I}{N} \quad \text{and} \quad g(I) = \hat{\beta} I, \tag{2}$$

where β is the frequency-dependent direct transmission rate and $\hat{\beta} = \frac{\beta}{S(0)}$ is the density-dependent direct transmission rate. Susceptible individuals can also become infected after contact with environmental zoospores by the environmental transmission functions $\rho c_m f(Z_m,\kappa_m)$ and $\rho c_e f(Z_e,\kappa_e)$ where c_m and c_e are the contact rate coefficients between individuals and environmental zoospores of type m and e, respectively, ρ is the percentage of these spores that successfully encyst, and

$$f(Z_i,\kappa_i) = \frac{Z_i}{Z_i+\kappa_i}; \quad i = m, e. \tag{3}$$

Here, κ_m and κ_e are the Bsal ID50s (the doses of each zoospore type needed to infect 50% of a population). Latently infected individuals $L(t)$ have an incubation duration of $1/\epsilon$, after which they become infectious $I(t)$. Infectious individuals have a disease induced mortality rate of δ and recover at rate γ. Once recovered, we assume that an individual becomes susceptible again at the loss of immunity rate η. Infectious individuals shed zoospore type Z_m at rate ω_m and zoospore type Z_e at rate ω_e. These environmental zoospores naturally degrade at rates ξ_m and ξ_e, respectively.

2.1.1 Basic Analysis of the Base Model

We assume that the initial solution of system (1) are non-negative, i.e.,

$$(S(0), L(0), I(0), R(0), Z_m(0), Z_e(0)) \geq (0, 0, 0, 0, 0). \tag{4}$$

The model is of the form $X' = F(X)$, $X(t_0) = X_0$ where $X_0 \in \mathbb{R}^n$ and $F : \mathbb{R}^n \to \mathbb{R}^n$ is C^1. Thus by the theorem 4.1 in [1] the solution exists and is unique.

The following lemmas show that the Base Model (1) with the assumed initial conditions (4) is biologically meaningful, as solutions are positive and bounded. The proofs are in Appendix 1.

Lemma 2.1 *The solutions* $(S(t), L(t), I(t), R(t), Z_m(t), Z_e(t))$ *of system (1) are nonnegative for all* $t \geq 0$ *with the nonnegative initial conditions (4) in* $\left(\mathbb{R}_0^+\right)^5$.

Lemma 2.2 *Let*

$$\Sigma_H = \left\{(S, L, I, R) \in \left(\mathbb{R}_0^+\right)^4 \mid 0 \leq S(t) + L(t) + I(t) + R(t) \leq N(0)\right\}$$

and

$$\Sigma_Z = \left\{(Z_m, Z_e) \in \left(\mathbb{R}_0^+\right)^2 \mid 0 \leq Z_m(t) + Z_e(t) \leq \frac{(\omega_m + \omega_e)N(0)}{\xi_m + \xi_e}\right\}.$$

Define

$$\Sigma = \Sigma_H \times \Sigma_Z.$$

If $Z(0) \leq \frac{(\omega_m+\omega_e)N(0)}{\xi_m+\xi_e}$, *then the region* Σ *is bounded for the model (1).*

2.2 Full Model Development

Infectious individuals in the base model (1) recover at constant rate γ. However, the probability of recovering from the infection should increase as an individual

progresses through the disease. Here, we update the base model so the probability of recovery increases the longer the individual resides in the infected compartment. Following [25], we divide the infection compartment into n subcompartments, where the rate of recovery to advance through each subcompartment is $n\gamma$. Here, the full model breaks up the infectious stage into a sequence of n subcompartments, each exponentially distributed with mean $1/(n\gamma)$. The number of infectious stages influences the distribution for the overall duration of the infectious period ranging from and exponential distribution when $n = 1$ to resembling gamma distributions when $n > 1$ [10]. This technique also allows for incorporating different parameters for transmission and zoospore shedding rates throughout the infectious period. The full model takes the following form:

$$\frac{dS}{dt} = -\underbrace{\sum_{i=1}^{n} g(I_i)\, S}_{\substack{\text{direct}\\ \text{transmission}}} - \underbrace{\rho(c_m f(Z_m, \kappa_m) + c_e f(Z_e, \kappa_e))S}_{\substack{\text{waterborne}\\ \text{transmission}}} + \underbrace{\eta R}_{\substack{\text{loss of}\\ \text{immunity}}} \tag{5a}$$

$$\frac{dL}{dt} = \underbrace{\sum_{i=1}^{n} g(I_i)\, S}_{\substack{\text{direct}\\ \text{transmission}}} + \underbrace{\rho(c_m f(Z_m, \kappa_m) + c_e f(Z_e, \kappa_e))S}_{\substack{\text{waterborne}\\ \text{transmission}}} - \underbrace{\epsilon L}_{\substack{\text{latent becomes}\\ \text{infectious}}} \tag{5b}$$

$$\frac{dI_1}{dt} = \underbrace{\epsilon L}_{\substack{\text{latent becomes}\\ \text{infectious}}} - \underbrace{\delta I_1}_{\substack{\text{disease induced}\\ \text{mortality}}} - \underbrace{n\gamma I_1}_{\substack{\text{infection}\\ \text{advances}}} \tag{5c}$$

$$\frac{dI_2}{dt} = \underbrace{n\gamma I_1}_{\substack{\text{infection}\\ \text{advances}}} - \underbrace{\delta I_2}_{\substack{\text{disease induced}\\ \text{mortality}}} - \underbrace{n\gamma I_2}_{\substack{\text{infection}\\ \text{advances}}} \tag{5d}$$

$$\vdots$$

$$\frac{dI_n}{dt} = \underbrace{n\gamma I_{n-1}}_{\substack{\text{infection}\\ \text{advances}}} - \underbrace{\delta I_n}_{\substack{\text{disease induced}\\ \text{mortality}}} - \underbrace{n\gamma I_n}_{\substack{\text{infection}\\ \text{advances}}} \tag{5e}$$

$$\frac{dR}{dt} = \underbrace{n\gamma I_n}_{\substack{\text{recovery}\\ \text{rate}}} - \underbrace{\eta R}_{\substack{\text{loss of}\\ \text{immunity}}} \tag{5f}$$

$$\frac{dZ_m}{dt} = \underbrace{\sum_{i=1}^{n} \omega_{mi} I_i}_{\substack{\text{shed}\\ \text{zoospores m}}} - \underbrace{\xi_m Z_m}_{\substack{\text{Bsal degradation}\\ \text{for zoospores m}}} \tag{5g}$$

$$\frac{dZ_e}{dt} = \underbrace{\sum_{i=1}^{n} \omega_{ei} I_i}_{\substack{\text{shed} \\ \text{zoospores e}}} - \underbrace{\xi_e Z_e}_{\substack{\text{Bsal degradation} \\ \text{for zoospores e}}}, \tag{5h}$$

where we incorporate multiple stages of infection (I_i) with varying direct transmission rates (β_i) and varying zoospores shedding rates (ω_{mi}, ω_{ei}) for $i = 1, ..., n$ stages of infection. Similar to the base model, direct transmission is either frequency dependent or density dependent, where the ith stage direct transmission function follows:

$$g(I_i) = \begin{cases} \beta_i \frac{I_i}{N} & \text{for frequency-dependent transmission} \\ \beta_i \frac{I_i}{S_0} = \hat{\beta}_i I_i & \text{for density-dependent transmission.} \end{cases} \tag{6}$$

The number of infectious stages, n, can play an important role in the model predictions; however, this also depends on the parameterization of $\beta_1, ..., \beta_n$, $\omega_{e1}, ..., \omega_{en}$, and $\omega_{m1}, ..., \omega_{mn}$. In order to compare how varying n influences the predictions, we normalized these parameters between the different cases while assuming that the transmission and zoospores shedding rates tend to increase as time post exposure increases. Here we use the following for setting the parameter values:

$$\beta_i = \beta_{\text{base}} \frac{2i}{n(n+1)}, \qquad \omega_{ei} = \omega_{e\text{base}} \frac{2i}{n(n+1)}, \quad \text{and} \quad \omega_{mi} = \omega_{m\text{base}} \frac{2i}{n(n+1)} \tag{7}$$

for $i = 1, 2, ...n$, so that $\sum_{i=1}^{n} \beta_i = \beta_{\text{base}}$, $\sum_{i=1}^{n} \omega_{ei} = \omega_{e\text{base}}$, and $\sum_{i=1}^{n} \omega_{mi} = \omega_{m\text{base}}$.

2.3 Parameterization

While adequately parameterizing models remains a major challenge in epidemic and ecology modeling, parameter sensitivity analyses help shed light on the relative importance of the parameters. This requires baseline values, as well as ranges for the parameter space. For our simulations, we used values from the eastern newt (when available), European fire salamander, and some results from the related chytrid fungus, B. dendrobatidis. Given the high transmission rates that have been reported [24], we assume a baseline direct transmission rate of $\beta_{\text{base}} = 2$ per day. Martel et al. [16] observed that infected salamanders died within 1 week after showing severe symptoms, therefore we set the disease induced mortality rate to $\delta = 0.14$ per day. Martel et al. [17] investigated the susceptibility of 34 amphibian species to Bsal and found in many species infection resulted in mortality of all infected animals and

other infected species had the possibility of recovery. Here, we allow the possibility of recovery and investigate a range of recovery rates $\gamma \in (0.05 - 0.9)$ per day with a waning immunity at rate $\eta \in (0.05, 1)$ per day. Stegen et al. [24] observed encysted zoospores persisted in the environmental for 1 month and were more resistant to predation that motile zoospores. Therefore, we assumed the baseline zoospore degradation rates of $\xi_e = 0.03$ per day and $\xi_m = 0.05$ per day. Zoospore shedding rates are unknown for Bsal in eastern newts, however, shedding rates have been measured for a similar fungal pathogen, Batrachochytrium dendrobatidis (Bd) in frogs [14]. Using these measured ranges of Bd zoospore shedding rate averaged across the frog species, we assumed $\omega_{mbase} \in (8.6 - 345)$ thousand zoospores per day. Additionally, we assumed that ω_{ebase} is half the value of ω_{mbase}. In some cases, parameter values are unknown, for example, contact rate coefficients with each type of environmental zoospores (c_m and c_e) and the percentage of contacted spores that successfully encyst (ρ). A summary of parameters and their assumed values is given in Table 1. Given the uncertainty of several parameters for the eastern newt systems, we focus our analyses on parameter sensitivity.

3 Full Model Analysis

Analysis of the above models includes parameter sensitivity analyses, numerical simulations, and calculation of the basic reproductive number. These results assume frequency-dependent transmission functions (Eqs. 2 and 6), however, density-dependent led to similar qualitative predictions and figures are not shown.

3.1 Parameter Sensitivity Analysis

Here, we use Latin hypercube sampling (LHS), developed by McKay et al. [19] with the statistical partial rank correlation coefficient (PRCC) technique in order to perform a sensitivity analysis of the parameter space of the full model (5). The LHS/PRCC sensitivity analysis method globally explores the multi-dimensional parameter space. LHS is a stratified Monte Carlo sampling without replacement technique that gives unbiased estimates of modeling output measures subject to combinations of varying parameters. The PRCC can be used to classify how the output measures are influences by changes in a specific parameter value, while linearly discounting the effects of the other parameters [15]. The PRCC is appropriate since each parameter has a monotonic relationship with the output measures, details given in the Appendix 3. Here, a positive PRCC has a positive relationship with the output measure, whereas a negative PRCC value has an inverse relationship with the output measure. Larger PRCC values do not necessarily indicate more important parameters, however, we used a z test on transformed PRCC values to rank model parameters in terms of relative sensitivity [15]. The number of

Table 1 Model parameters

	Parameter	Unit	Base value	Range	Source
β_{base}	Base direct transmission rate	1/day	2	(0.1, 3)	[24][a]
c_m	Environmental contact rate coefficient with Z_m	1/day	0.02	(0.01, 0.05)	Assumed
c_e	Environmental contact rate coefficient with Z_e	1/day	0.01	(0.005, 0.03)	Assumed
η	Loss of immunity rate	1/day	0.1	(0.05, 1)	[13, 17][b]
$1/\epsilon$	Latency period	Days	10	(7, 14)	[13, 17][b]
δ	Disease induced mortality rate	1/day	0.14	(0.01, 0.5)	[13, 16, 17][b]
γ	Bsal recovery rate	1/day	0.1	(0.05, 0.9)	[13, 17][b]
n	Number of infected stages	–	5	NA	Assumed
ρ	% of contacted spores that encyst	–	0.75	(0.5, 1)	Assumed
$\omega_{m\text{base}}$	Base shedding rate of Z_m	$\frac{1000Zoospores}{day.individual}$	176	(8.6–345)	[14][c]
$\omega_{e\text{base}}$	Base shedding rate of Z_e	$\frac{1000Zoospores}{day.individual}$	88	(4.3–172)	Assumed $\omega_{e\text{base}} = \frac{1}{2}\omega_{m\text{base}}$
ξ_m	Degradation rate of Z_m	1/day	0.05	(0.02, 2)	[24][a]
ξ_e	Degradation rate of Z_e	1/day	0.03	(0.01, 1)	[24][a]
κ_m	ID-50	$\frac{Zoospore}{Vol}$	245K	(240K–250K)	MJG, unpublished data[b]
κ_e	ID-50	$\frac{Zoospore}{Vol}$	145K	(140K–150K)	Assumed $\kappa_e < \kappa_m$

[a]Values from *Salamandra salamandra* data
[b]Values from *Notophthalmus viridescens* data
[c]Values obtained from Bd (*Batrachochytrium dendrobatidis*) data

model simulations (or runs $= R$) need to be $\frac{4}{3}$ times greater than the number of uncertain parameters k, i.e., $R > \frac{4}{3}k$ [2, 5]. Our parameter space consist of 26 parameters and we choose 5,000 runs for our simulations. We used two output measures to classify the sensitivity of the parameters which has the monotone relation with our input variables;

1. The size of the Newt population after 150 days,
2. The maximum load of environmental zoospores at any time of the simulation 150 days.

The choice of using 150 days for the length of the simulations was to ensure the environmental zoospores concentrations achieved their maximum during the simulations. This duration also is within the expected duration to observe population collapse due to Bsal invasion in highly susceptible species [24]. The PRCC values for the Newt population density are shown in Fig. 3 and the PRCC values for the maximum zoospore load are shown in Fig. 4.

Figure 3 illustrates the most sensitive parameters affecting the size of the newt population. The Newt population increased significantly for increases in recovery rate γ. The Newt population decreased for increases in the direct transmission rates (β_i), the loss of immunity (η), the rate an infected individual becomes infectious (ϵ, inverse of the incubation period), as well as the disease induced mortality rate (δ).

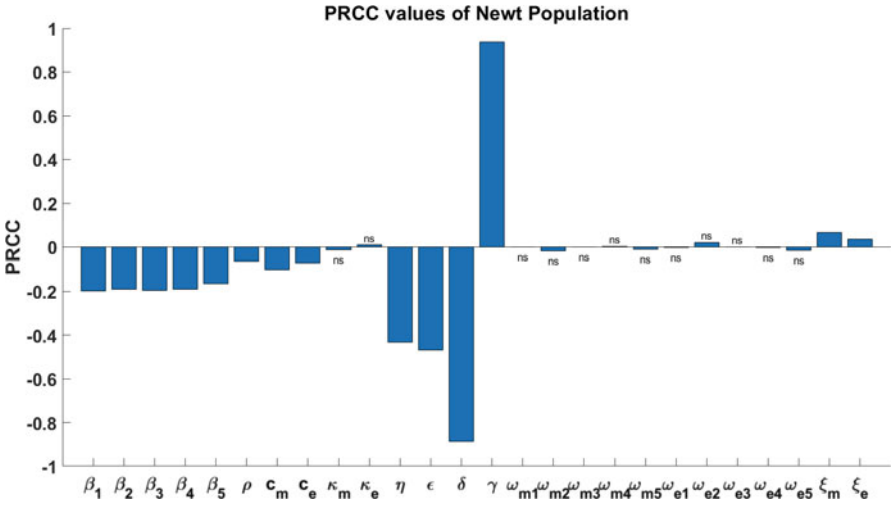

Fig. 3 Partial rank correlation coefficient (PRCC) values for each parameter in the Latin hypercube sampling (LHS) using the surviving Newt population density after 150 days as the output measure. Values marked ns are non-significant ($P > 0.05$)

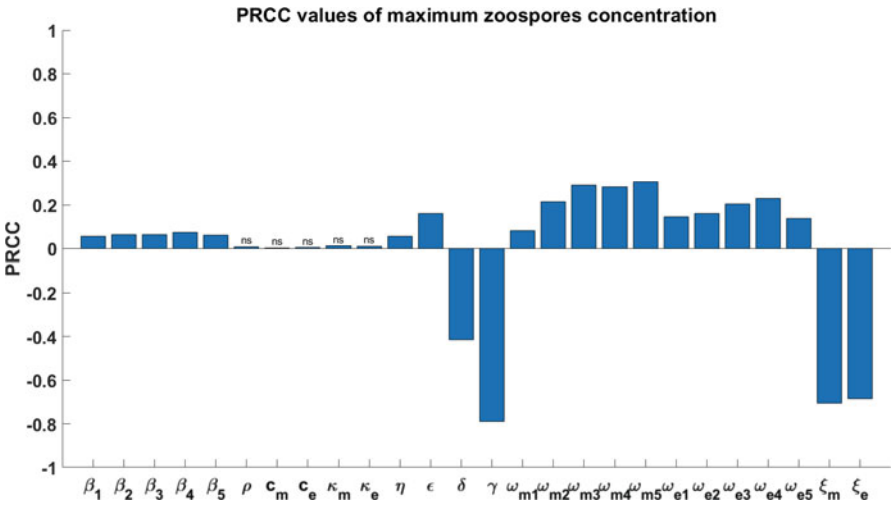

Fig. 4 Partial rank correlation coefficient (PRCC) values for each parameter in the Latin hypercube sampling (LHS) using maximum environmental zoospore load after 150 days as the output measure. Values marked ns are non-significant ($P > 0.05$)

For the maximum environmental zoospore load (Fig. 4), the zoospores concentration increased significantly for shorter incubation periods $1/\epsilon$ (i.e., larger the rate at which an infected individual becomes infectious, ϵ) and high zoospore shedding rates (ω_{mi} and ω_{ei} for $i = 1, ..., 5$). The zoospore concentration decreased significantly with larger disease induced mortality and recovery rates (δ, γ) as well as higher rates of environmental zoospore degradation (ξ_m and ξ_e).

3.2 Numerical Simulations

We varied the recovery rate (γ) to study the effect on the total Newt population, the final epidemic size, and the total maximum zoospores concentrations. The final epidemic size was calculated as the total number of cases over the duration of the simulation (150 days). As γ increased, a larger portion of the population survived the outbreak (Fig. 5a) and total maximum zoospores concentration decreased (Fig. 6). While an increase in γ increased survival of the population (Fig. 5a) it also increased the final epidemic size (Fig. 5b).

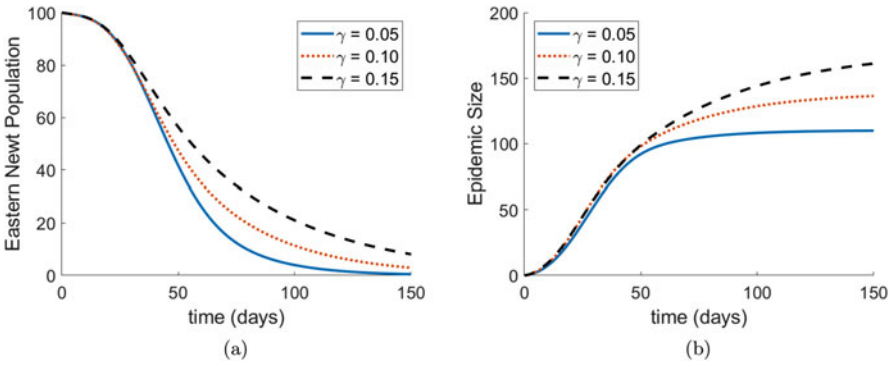

Fig. 5 (**a**) Eastern newt population and (**b**) endemic size for varying the recovery rate, γ and all other parameters are set to the baseline values from Table 1

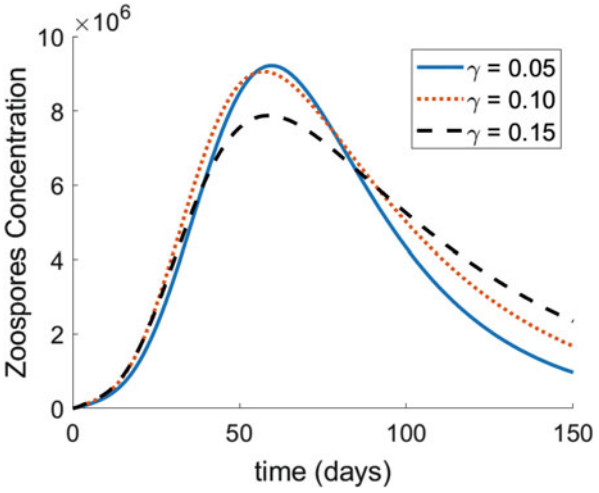

Fig. 6 Total maximum zoopores concentration varying the recovery rate, γ and all other parameters are set to the baseline values from Table 1

Varying the incubation period $(1/\epsilon)$, the model predicted that the newt population decreased only slightly for shorter period, however, the total maximum zoospores concentration increased substantially (Figs. 7 and 8).

We also investigated the influence of disease induced mortality rates (δ). While increases in δ decreased the newt population and the epidemic size (Fig. 9), it also caused a decrease in the zoospore concentration (Fig. 10).

Variations in the degradation rates of zoopores (ξ_e, ξ_m) did not substantially affect the newt population size (Fig. 11), however, it did play an important role in environmental zoospore loads (Fig. 12).

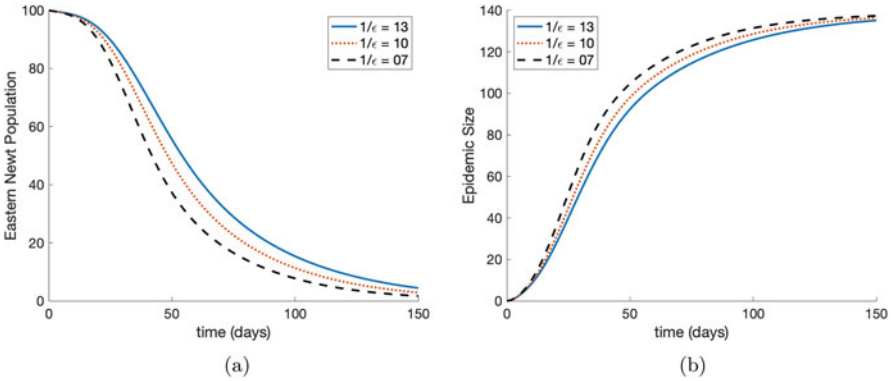

Fig. 7 (**a**) Eastern newt population and (**b**) epidemic size for varying the latency period, $1/\epsilon$ and all other parameter are set to the baseline values from Table 1

Fig. 8 Total maximum zoospores concentration varying the latency period, $1/\epsilon$ and all other parameters are set to the baseline values from Table 1

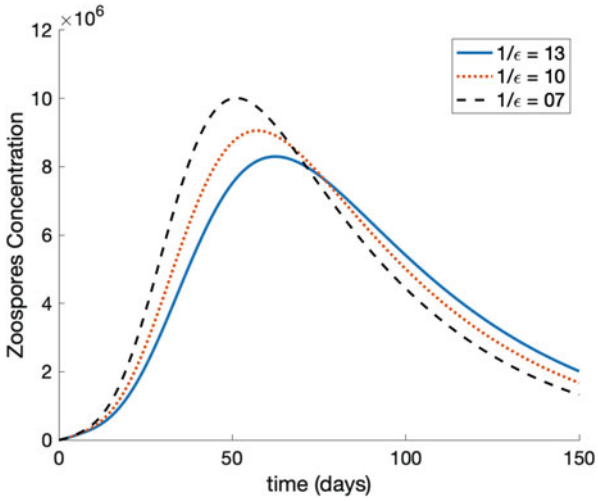

Figure 13 showed how varying the number of infectious stages n influenced model predictions. For smaller n the outbreak occurred earlier as the peak number of infected cases occurred sooner and was higher in magnitude (Fig. 13a, b). Additionally, for higher n the maximum zoospore concentration was delayed and was lower in magnitude (Fig. 13c).

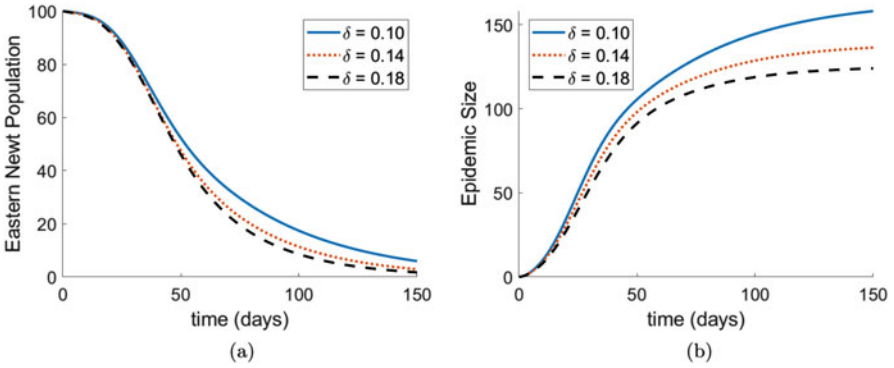

Fig. 9 (**a**) Eastern newt population and (**b**) epidemic size for varying the disease induced mortality rate δ and all other parameter are set to the baseline values from Table 1

Fig. 10 Total maximum zoospores concentration varying the disease induced mortality rate, $1/\delta$ and all other parameters are set to the baseline values from Table 1

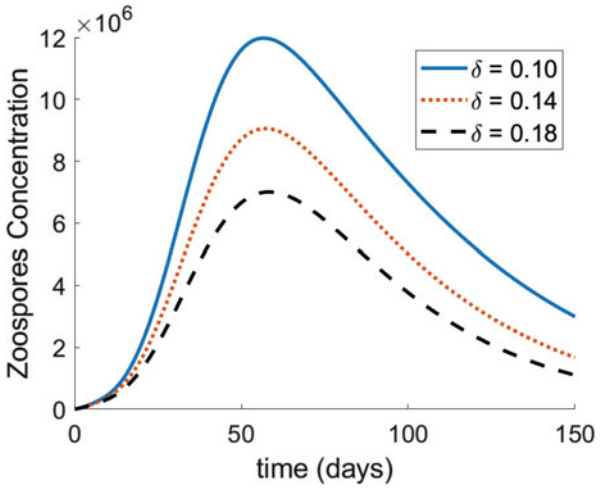

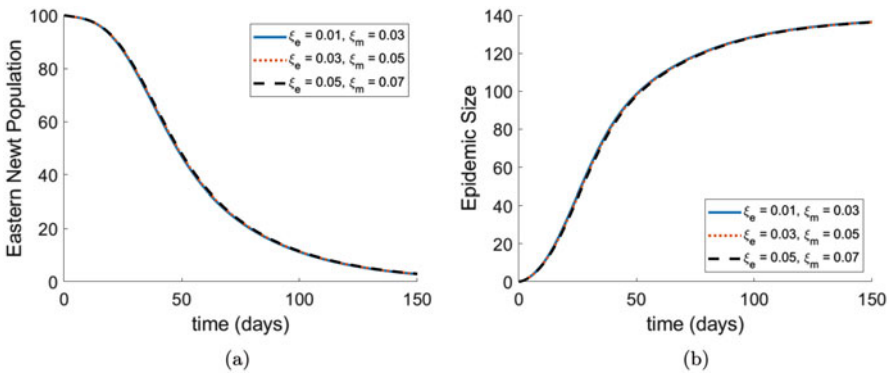

Fig. 11 (**a**) Eastern newt population and (**b**) epidemic size for varying the degradation rates of zoopores (ξ_e, ξ_m) and all other parameter are set to the baseline values from Table 1

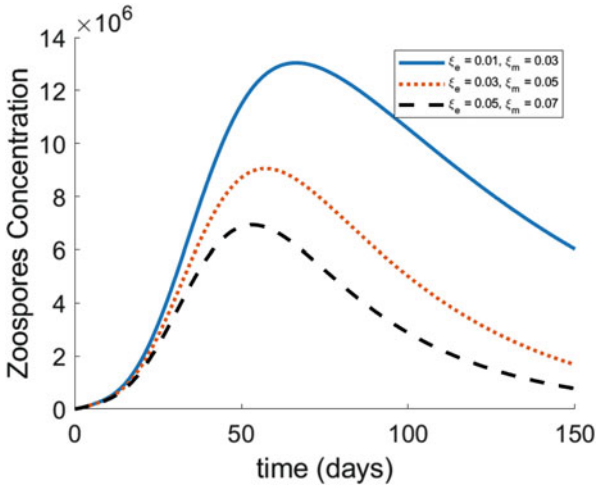

Fig. 12 Total maximum zoospores concentration varying the degradation rates of zoopores (ξ_e, ξ_m) and all other parameters are set to the baseline values from Table 1

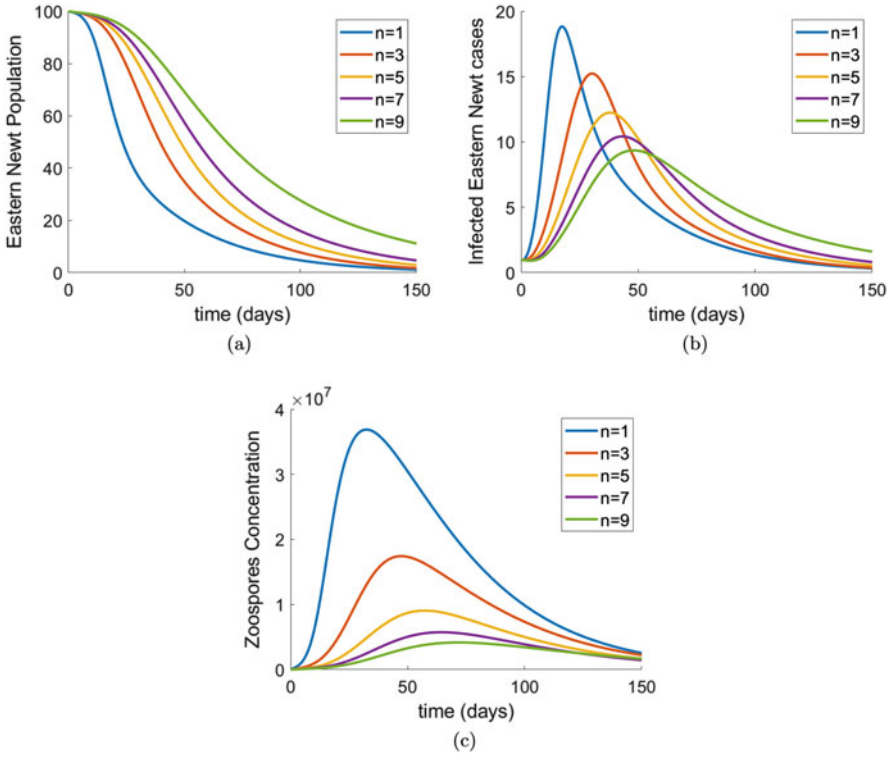

Fig. 13 (**a**) Eastern newt population (**b**) total infected eastern newt population, and (**c**) zoospores concentration for varying number of infectious stages, n using equation (7) for β_i, ω_{ei}, and ω_{mi} with all other parameters set to the baseline values in Table 1

3.3 Basic Reproductive Number

The basic reproduction number $\mathcal{R}_0$ is the expected number of secondary infections in a completely susceptible population produced by a single infectious individual during its infectious period [3]. To derive the basic reduction number, $\mathcal{R}_0$ of Bsal, we use the next-generation matrix approach for the system (5) following [4]. The analytic expression of the basic reproduction number $\mathcal{R}_0$ is as follows and the details are shown in the Appendix 2.

$$\mathcal{R}_0 = \underbrace{\sum_{i=1}^{n} \beta_i \overbrace{\left(\frac{\gamma n}{\delta+\gamma n}\right)^{i-1}}^{\text{fraction survives to the } i^{th} \text{ stage}} \overbrace{\frac{1}{\delta+\gamma n}}^{\text{duration in the } i^{th} \text{ stage}}}_{\text{direct}} + \underbrace{\frac{\rho c_m S_0 \sum_{i=1}^{n} \omega_{mi} (\gamma n)^{i-1} (\delta+\gamma n)^{n-i}}{(\delta+\gamma n)^n \xi_m \kappa_m}}_{\text{environmental for zoospores m}}$$

$$+ \underbrace{\frac{\rho c_e S_0 \sum_{i=1}^{n} \omega_{ei} (\gamma n)^{i-1} (\delta+\gamma n)^{n-i}}{(\delta+\gamma n)^n \xi_e \kappa_e}}_{\text{environmental for zoospores e}}, \tag{8}$$

where S_0 is the initial number of susceptible individuals. All transmission pathways contribute to the analytical expression of $\mathcal{R}_0$ which is a measure of potential outbreak. The expression in Eq. (8) describes the relative contribution of each pathway. We investigate the relative contributions of each pathway to $\mathcal{R}_0$ in order to identify the dominant pathway.

The dominant pathway depends on the population size (Table 2, Fig. 14). Direct transmission is the dominant pathway for small populations sizes (population size <5). As the population size increases (population size >5), environmental transmission for Z_m becomes the dominant pathway, while the environmental pathway for Z_e remains subordinate. As populations sized continue to increase (>7) then the directed transmission pathway becomes subordinate.

Table 2 Numerical values of $\mathcal{R}_0$ using parameter values from Table 1

	$S_0 = 1$	$S_0 = 5$	$S_0 = 7$	$S_0 = 30$
Total $\mathcal{R}_0$	1.15	2.35	2.95	9.84
Direct contact transmission proportion of $\mathcal{R}_0$	0.74	0.36	0.29	0.09
Environmental transmission proportion of $\mathcal{R}_0$ (Z_m)	0.16	0.39	0.43	0.55
Environmental transmission proportion of $\mathcal{R}_0$ (Z_e)	0.10	0.25	0.28	0.36

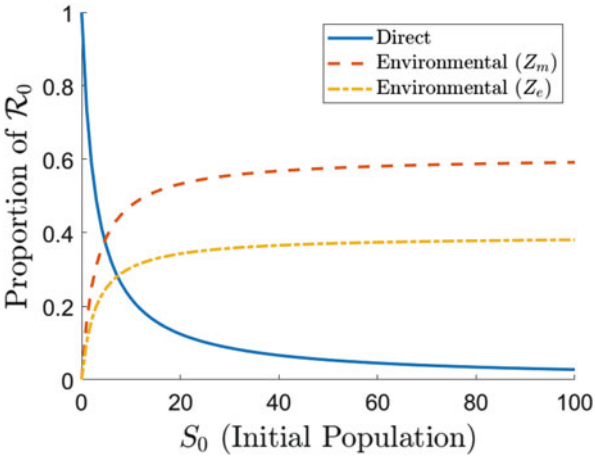

Fig. 14 Proportion of $\mathcal{R}_0$ for each transmission pathway given in Eq. (8) using parameter values from Table 1

4 Discussion

Infection disease models offer a powerful tool to better understand and predict epidemics in human and ecological systems. Bsal is an emerging infectious pathogen with potentially devastating biodiversity crisis in North America [26]. To better understand the dynamics, we developed and analyzed the first model of the highly virulent emerging pathogen Bsal on a host population of Eastern Newts that incorporates multiple transmission pathways with multiple stages of infection. The model predicts significant declines in host population shown in Fig. 5. These predictions are qualitatively consistent with empirical data captured by Stegen et al. [24], which show a collapse of 90% of a population of salamander introduced to Bsal within 6 months.

While varying key parameters can slow down population declines, the pathogen will persist as the basic reproduction number is always greater than one (Table 2). While previous models have concluded that mitigation during outbreaks is likely to fail and control efforts should focus on preventing disease emergence [23], once Bsal is established in an area, slowing the spread may help prevent nearby populations from being exposed.

Model predictions are sensitive to the number of infectious stages incorporated in the model structure (Fig. 13). Fitting the model to empirical data can help better parameterize the number of stages. For example, [20] fit a similar model to empirical data of Ranavirus cases in wood frogs Peace et al. [20].

The analytical expression of the basic reproductive number $\mathcal{R}_0$ given in Eq. (8) was used to identify the dominant transmission pathway. Our model and parameter set predicts that direct transmission is the dominant pathway for small population densities, however, environmental transmission is the dominant pathway for large population densities. These results can help guide intervention strategies. For example, in small density scenarios where direct transmission is the dominant pathway, we suggest intervention strategies focus efforts on reducing the contact rate between individuals. This can be done by increasing habitat complexity among them such as aquatic plants. For larger population densities, the model suggests that more efficient diseased control strategies would be to reduce environmental transmission. Here, the parameters that have the largest influence the maximum environmental zoospores concentrations (high PRCC values in Fig. 4) should be the main focus of intervention strategies. For example, the degradation rate of the zoospores in the environment have large influence on epidemic dynamics, which suggests the use of intervention strategies to increase ξ_m and ξ_e such as increasing UV penetration or number of zooplankton in the water [24] might reduce zoospore persistence.

The developed models consider a homogeneous population of Eastern Newts, however, disease dynamics for each individual is like to depend on their life stage (larvae, juvenile, adult). A future iteration of the model should consider a heterogeneous population and include stage structure of the host population. While our parameter sensitivity analysis highlights the important role that recovery rates can have, many species may have very low or zero probabilities of recovering from Bsal [17]. Given the hyper-susceptibility of eastern newts and fire salamanders to Bsal chytridiomycosis [17], it is possible that our simulations represent plausible scenarios in North America if Bsal in introduced. It is also possible that seasonal variations can influence disease and population dynamics, hence future iterations of the model should consider how temperature influences host contact rates, zoospore persistence, and importance of transmission pathways.

Appendix 1: Proofs of Base Model Lemmas

Proof of Lemma 2.1:

Proof We have

$$\left.\frac{dS}{dt}\right|_{\alpha(S)} = \eta R > 0$$

$$\left.\frac{dL}{dt}\right|_{\alpha(L)} = g(I)\,S + \rho(c_m f(Z_m, \kappa_m) + c_e f(Z_e, \kappa_e))S > 0$$

$$\left.\frac{dI}{dt}\right|_{\alpha(I)} = \epsilon L > 0$$

$$\left.\frac{dR}{dt}\right|_{\alpha(R)} = \gamma I > 0$$

$$\left.\frac{dZ_m}{dt}\right|_{\alpha(Z_m)} = \omega_m I > 0$$

$$\left.\frac{dZ_e}{dt}\right|_{\alpha(Z_e)} = \omega_e I > 0,$$

where $\alpha(x) = \{x(t) = 0$ and $S, L, I, R, Z_m, Z_e \in C(\mathbb{R}_0^+, \mathbb{R}_0^+)\}$ and $x \in \{S, L, I, R, Z_m, Z_e\}$. Therefore, due to the Lemma (2) in [7], any solutions $(S(t), L(t), I(t), R(t), Z_m(t), Z_e(t))$ of system (1) are nonnegative for all $t \geq 0$ with the nonnegative initial conditions (4) in $\left(\mathbb{R}_0^+\right)^5$.

Proof of Lemma 2.2:

Proof We can divide our system (1) into two parts: the host population, $N'(t) = S'(t) + L'(t) + I'(t) + R'(t)$ and the zoospores population, $Z(t) = Z_m(t) + Z_e(t)$. Adding the first four equations of system (1) yields

$$N'(t) = S'(t) + L'(t) + I'(t) + R'(t) = -\delta I \leq 0$$

which is a decreasing function of time. Therefore, $N(t) \leq N(0)$ and adding the last two equations of system (1) yields

$$Z'(t) = Z_m'(t) + Z_e'(t) = (\omega_m + \omega_e)I(t) - (\xi_m + \xi_e)Z(t)$$

$$\leq (\omega_m + \omega_e)N(0) - (\xi_m + \xi_e)Z(t).$$

A standard comparison theorem in [11] can be used to show that

$$Z(t) \leq Z(0)e^{-(\xi_m+\xi_e)t} + \frac{(\omega_m + \omega_e)N(0)}{(\xi_m + \xi_e)}(1 - e^{-(\xi_m+\xi_e)t})$$

$$= \frac{(\omega_m + \omega_e)N(0)}{(\xi_m + \xi_e)} + \left(Z(0) - \frac{(\omega_m + \omega_e)N(0)}{(\xi_m + \xi_e)}\right)e^{-(\xi_m+\xi_e)t}.$$

Therefore, if $Z(0) \leq \frac{(\omega_m+\omega_e)N(0)}{(\xi_m+\xi_e)}$, then $Z(t) \leq \frac{(\omega_m+\omega_e)N(0)}{(\xi_m+\xi_e)}$. Thus the region Σ is bounded.

Appendix 2: Basic Reproduction Number

The Jacobian matrix J of the system (5) is obtained from linearizing the system. Model (5) has a disease-free equilibria at $\mathbf{X}_0 = (S_0, \ldots, 0, 0)$, where S_0 is the initial population of susceptible individuals. Evaluating the Jacobian matrix at $\mathbf{X}_0$ yields

$$\mathbf{J} = \begin{pmatrix}
0 & 0 & -\beta_1 & -\beta_2 & \ldots & -\beta_{n-1} & -\beta_n & \eta & -\frac{\rho c_m S_0}{\kappa_m} & -\frac{\rho c_e S_0}{\kappa_e} \\
0 & -\epsilon & \beta_1 & \beta_2 & \ldots & \beta_{n-1} & \beta_n & 0 & \frac{\rho c_m S_0}{\kappa_m} & \frac{\rho c_e S_0}{\kappa_e} \\
0 & \epsilon & -n\gamma - \delta & 0 & \ldots & 0 & 0 & 0 & 0 & 0 \\
0 & 0 & n\gamma & -n\gamma - \delta & \ldots & 0 & 0 & 0 & 0 & 0 \\
0 & 0 & 0 & n\gamma & \ldots & 0 & 0 & 0 & 0 & 0 \\
0 & 0 & 0 & 0 & \ldots & -n\gamma - \delta & 0 & 0 & 0 & 0 \\
0 & 0 & 0 & 0 & \ldots & n\gamma & -n\gamma - \delta & 0 & 0 & 0 \\
0 & 0 & 0 & 0 & \ldots & 0 & n\gamma & -\eta & 0 & 0 \\
0 & 0 & \omega_{m1} & \omega_{m2} & \ldots & \omega_{m(n-1)} & \omega_{mn} & 0 & -\xi_m & 0 \\
0 & 0 & \omega_{e1} & \omega_{e2} & \ldots & \omega_{e(n-1)} & \omega_{en} & 0 & 0 & -\xi_e.
\end{pmatrix}$$

Near the $\mathbf{X}_0$, for small perturbations $\mathbf{z} = (L, I_1, I_2, \ldots, I_n, R, Z_m, Z_e)$ the linearized infected subsystem of (5) evolves according to the following system of equations:

$$\frac{\mathrm{d}\mathbf{z}}{\mathrm{dt}} = \mathbf{M}\,\mathbf{z},$$

where

$$\mathbf{M} = \begin{pmatrix}
-\epsilon & \beta_1 & \beta_2 & \ldots & \beta_{n-1} & \beta_n & 0 & \frac{\rho c_m S_0}{\kappa_m} & \frac{\rho c_e S_0}{\kappa_e} \\
\epsilon & -n\gamma - \delta & 0 & \ldots & 0 & 0 & 0 & 0 & 0 \\
0 & n\gamma & -n\gamma - \delta & \ldots & 0 & 0 & 0 & 0 & 0 \\
0 & 0 & n\gamma & \ldots & 0 & 0 & 0 & 0 & 0 \\
0 & 0 & 0 & \ldots & -n\gamma - \delta & 0 & 0 & 0 & 0 \\
0 & 0 & 0 & \ldots & n\gamma & -n\gamma - \delta & 0 & 0 & 0 \\
0 & 0 & 0 & \ldots & 0 & n\gamma & -\eta & 0 & 0 \\
0 & \omega_{m1} & \omega_{m2} & \ldots & \omega_{m(n-1)} & \omega_{mn} & 0 & -\xi_m & 0 \\
0 & \omega_{e1} & \omega_{e2} & \ldots & \omega_{e(n-1)} & \omega_{en} & 0 & 0 & -\xi_e.
\end{pmatrix}$$

We decompose the matrix $\mathbf{M}$ into transmission ($\mathbf{T}$) and transition ($\boldsymbol{\Sigma}$) matrices, respectively, obtaining

$$\frac{\mathrm{d}\mathbf{z}}{\mathrm{dt}} = (\mathbf{T} + \boldsymbol{\Sigma})\,\mathbf{z},$$

where

$$\mathbf{T} = \begin{pmatrix} 0 & \beta_1 & \beta_2 & \dots & \beta_{n-1} & \beta_n & 0 & \frac{\rho c_m S_0}{\kappa_m} & \frac{\rho c_e S_0}{\kappa_e} \\ 0 & 0 & 0 & \dots & 0 & 0 & 0 & 0 & 0 \\ 0 & 0 & 0 & \dots & 0 & 0 & 0 & 0 & 0 \\ 0 & 0 & 0 & \dots & 0 & 0 & 0 & 0 & 0 \\ 0 & 0 & 0 & \dots & 0 & 0 & 0 & 0 & 0 \\ 0 & 0 & 0 & \dots & 0 & 0 & 0 & 0 & 0 \\ 0 & 0 & 0 & \dots & 0 & 0 & 0 & 0 & 0 \\ 0 & 0 & 0 & \dots & 0 & 0 & 0 & 0 & 0 \\ 0 & 0 & 0 & \dots & 0 & 0 & 0 & 0 & 0 \end{pmatrix}$$

and

$$\boldsymbol{\Sigma} = \begin{pmatrix} -\epsilon & 0 & 0 & \dots & 0 & 0 & 0 & 0 & 0 \\ \epsilon & -n\gamma - \delta & 0 & \dots & 0 & 0 & 0 & 0 & 0 \\ 0 & n\gamma & -n\gamma - \delta & \dots & 0 & 0 & 0 & 0 & 0 \\ 0 & 0 & n\gamma & \dots & 0 & 0 & 0 & 0 & 0 \\ 0 & 0 & 0 & \dots & -n\gamma - \delta & 0 & 0 & 0 & 0 \\ 0 & 0 & 0 & \dots & n\gamma & -n\gamma - \delta & 0 & 0 & 0 \\ 0 & 0 & 0 & \dots & 0 & n\gamma & -\eta & 0 & 0 \\ 0 & \omega_{m1} & \omega_{m2} & \dots & \omega_{m(n-1)} & \omega_{mn} & 0 & -\xi_m & 0 \\ 0 & \omega_{e1} & \omega_{e2} & \dots & \omega_{e(n-1)} & \omega_{en} & 0 & 0 & -\xi_e. \end{pmatrix}$$

The next-generation matrix with large domain is $\mathbf{K} = -\mathbf{T}\boldsymbol{\Sigma}^{-1}$. Since $\mathbf{T}$ has rank 1, the NGM $\mathbf{K}$ also has rank 1. Therefore, only the first row of $\mathbf{K}$ contains non-zero entries. Consequently, the spectral radius of $\mathbf{K}$ is the first entry on the diagonal, i.e., $\mathbf{K}_{1,1}$ which is equivalent to $\mathcal{R}_0$, and it is the same for both frequency and density-dependent direct transmission. Therefore,

$$\mathcal{R}_0 = \underbrace{\sum_{i=1}^{n} \beta_i \overbrace{\left(\frac{\gamma n}{\delta+\gamma n}\right)^{i-1}}^{\text{fraction survives to the } i^{th} \text{ stage}} \overbrace{\frac{1}{\delta+\gamma n}}^{\text{duration in the } i^{th} \text{ stage}}}_{\text{direct}} + \underbrace{\frac{\rho c_m S_0 \sum_{i=1}^{n} \omega_{mi} (\gamma n)^{i-1} (\delta+\gamma n)^{n-i}}{(\delta+\gamma n)^n \xi_m \kappa_m}}_{\text{environmental for zoospores m}}$$

$$+ \underbrace{\frac{\rho c_e S_0 \sum_{i=1}^{n} \omega_{ei} (\gamma n)^{i-1} (\delta+\gamma n)^{n-i}}{(\delta+\gamma n)^n \xi_e \kappa_e}}_{\text{environmental for zoospores e}},$$

where S_0 is the initial number of susceptible individuals.

Appendix 3: Monotonicity Test

Each subplot of the following Figs. 15 and 16 shows the monotonic relation between the model parameters with the output variable Eastern Newt population and maximum Zoospores concentrations, respectively, which is a required condition for the PRCC-LHS test.

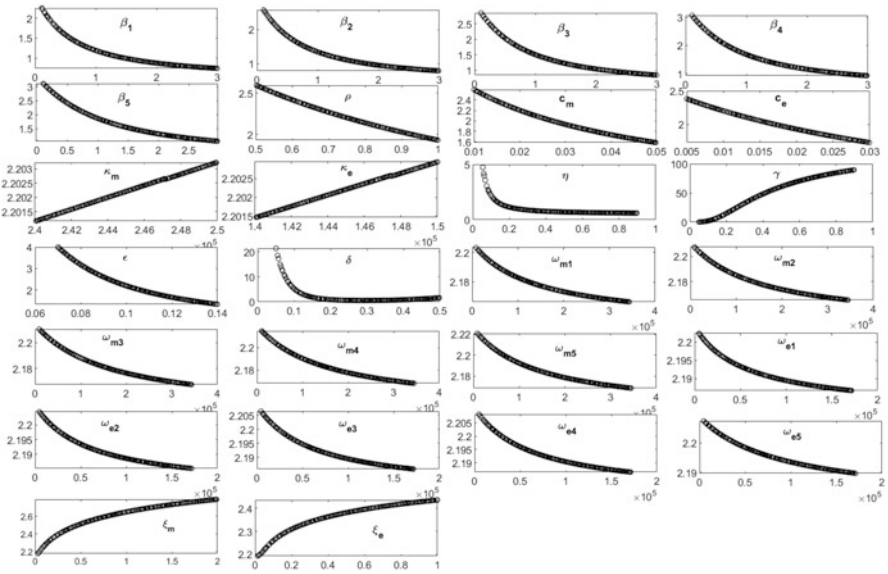

Fig. 15 Monotonicity plot of the model parameters vs. the output measure eastern newt population

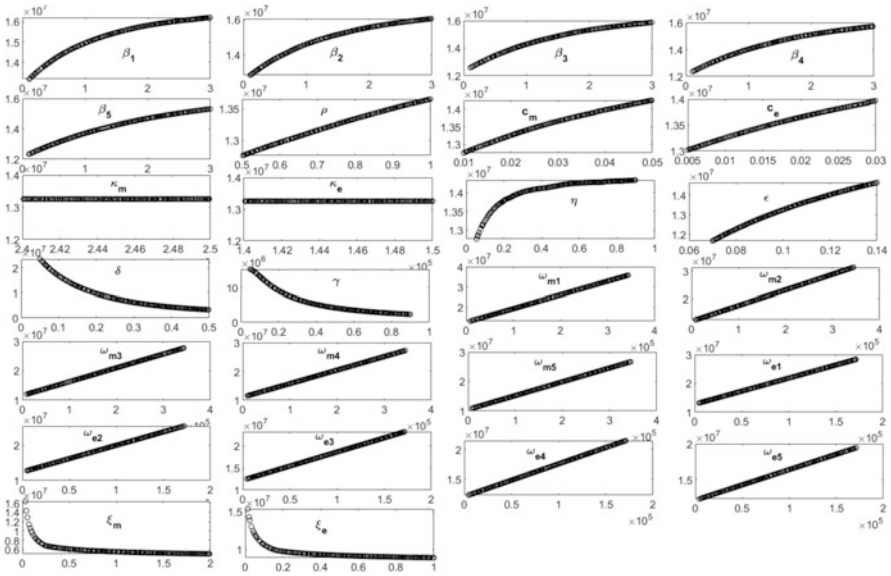

Fig. 16 Monotonicity plot of the model parameters vs. the output measure total maximum zoospores concentration

References

1. Allen, L.J.: Introduction to Mathematical Biology. Pearson, London/Prentice Hall, Upper Saddle River (2007)
2. Blower, S.M., Dowlatabadi, H.: Sensitivity and uncertainty analysis of complex models of disease transmission: an HIV model, as an example. Int. Stat. Rev. **62**, 229–243 (1994)
3. Diekmann, O., Heesterbeek, J.A.P., Metz, J.A.: On the definition and the computation of the basic reproduction ratio r 0 in models for infectious diseases in heterogeneous populations. J. Math. Bio. **28**(4), 365–382 (1990)
4. Diekmann, O., Heesterbeek, J.A.P., Roberts, M.G.: The construction of next-generation matrices for compartmental epidemic models. J. R. Soc. Interface **7**(47), 873–885 (2010)
5. Gomero, B.: Latin hypercube sampling and partial rank correlation coefficient analysis applied to an optimal control problem. Master's Thesis, University of Tennessee (2012)
6. Gray, M.J., Lewis, J.P., Nanjappa, P., Klocke, B., Pasmans, F., Martel, A., Stephen, C., Olea G.P., Smith, S.A., Sacerdote-Velat, A., et al.: Batrachochytrium salamandrivorans: the North American response and a call for action. PLoS Path. **11**(12), e1005251 (2015)
7. Huo, H.F.: Permanence and global attractivity of delay diffusive prey-predator systems with the michaelis-menten functional response. Comput. Math. Appl. **49**(2-3), 407–416 (2005)
8. Katz, T.S., Zellmer, A.J.: Comparison of model selection technique performance in predicting the spread of newly invasive species: a case study with batrachochytrium salamandrivorans. Biol. Invasions **20**(8), 2107–2119 (2018)
9. Keeling, M.J., Rohani, P.: Modeling Infectious Diseases in Humans and Animals. Princeton University Press, Princeton (2011)
10. Krylova, O., Earn, D.J.: Effects of the infectious period distribution on predicted transitions in childhood disease dynamics. J. R. Soc. Interface **10**(84), 20130098 (2013)

11. Lakshmikantham, V., Leela, S., Martynyuk, A.A.: Stability Analysis of Nonlinear Systems. Springer, Berlin (1989)
12. Lloyd, A.L.: Destabilization of epidemic models with the inclusion of realistic distributions of infectious periods. Proc. R. Soc. Lond. B Biol. Sci. **268**(1470), 985–993 (2001)
13. Longo, A.V., Fleischer, R.C., Lips, K.R.: Double trouble: co-infections of chytrid fungi will severely impact widely distributed newts. Biol. Invasions **21**(6), 2233–2245 (2019)
14. Maguire, C., DiRenzo, G.V., Tunstall, T.S., Muletz, C.R., Zamudio, K.R., Lips, K.R.: Dead or alive? Viability of chytrid zoospores shed from live amphibian hosts. Dis. Aquat. Organ. **119**(3), 179–187 (2016)
15. Marino, S., Hogue, I.B., Ray, C.J., Kirschner, D.E.: A methodology for performing global uncertainty and sensitivity analysis in systems biology. J. Theor. Bio. **254**(1), 178–196 (2008)
16. Martel, A., Spitzen-van der Sluijs, A., Blooi, M., Bert, W., Ducatelle, R., Fisher, M.C., Woeltjes, A., Bosman, W., Chiers, K., Bossuyt, F., et al: Batrachochytrium salamandrivorans sp. nov. causes lethal chytridiomycosis in amphibians. Proc. Natl. Acad. Sci. **110**(38), 15325–15329 (2013)
17. Martel, A., Blooi, M., Adriaensen, C., Van Rooij, P., Beukema, W., Fisher, M.C., Farrer, R.A., Schmidt, B.R., Tobler, U., Goka, K., et al.: Recent introduction of a chytrid fungus endangers western Palearctic salamanders. Science **346**(6209), 630–631 (2014)
18. McCraw, S., Gurr, S.: Emerging fungal threats to animal, plant and ecosystem health. Nature **484**(7393), 186194 (2012)
19. McKay, M.D., Beckman, R.J., Conover, W.J.: A comparison of three methods for selecting values of input variables in the analysis of output from a computer code. Technometrics **42**(1), 55–61 (2000)
20. Peace, A., O'Regan, S.M., Spatz, J.A., Reilly, P.N., Hill, R.D., Carter, E.D., Wilkes, R.P., Waltzek, T.B., Miller, D.L., Gray, M.J.: A highly invasive chimeric ranavirus can decimate tadpole populations rapidly through multiple transmission pathways. Ecol. Model. **410**, 108777 (2019)
21. Petranka, J.W.: Salamanders of the United States and Canada. Smithsonian Institution Press, Washington (1998)
22. Roe, A.W., Grayson, K.L.: Terrestrial movements and habitat use of juvenile and emigrating adult eastern red-spotted newts, notophthalmus viridescens. J. Herpetol. **42**(1), 22–31 (2008)
23. Schmidt, B.R., Bozzuto, C., Lötters, S., Steinfartz, S.: Dynamics of host populations affected by the emerging fungal pathogen batrachochytrium salamandrivorans. R. Soc. Open Sci. **4**(3), 160801 (2017)
24. Stegen, G., Pasmans, F., Schmidt, B.R., Rouffaer, L.O., Van Praet, S., Schaub, M., Canessa, S., Laudelout, A., Kinet, T., Adriaensen, C., et al.: Drivers of salamander extirpation mediated by batrachochytrium salamandrivorans. Nature **544**(7650), 353–356 (2017)
25. Wearing, H.J., Rohani, P., Keeling, M.J.: Appropriate models for the management of infectious diseases. PLoS Med. **2**(7), 621 (2005)
26. Yap, T.A., Koo, M.S., Ambrose, R.F., Wake, D.B., Vredenburg, V.T.: Averting a North American biodiversity crisis. Science **349**(6247), 481–482 (2015)